CHAPTER II

LITERATURE REVIEW

2.1. Background on Polyolefin Catalysts

Polyolefins can be produced with free radical initiators, Phillips type catalysts, Ziegler-Natta catalysts and metallocene catalysts. Ziegler-Natta catalysts have been most widely used because of their broad range of application. However, Ziegler-Natta catalyst provides polymers having broad molecular weight distribution (MWD) and composition distribution due to multiple active sites formed [9].

Metallocene catalysts have been used to polymerize ethylene and α-olefins commercially. The structural change of metallocene catalysts can control composition distribution, incorporation of various comonomers, MWD and stereoregularity [10].

2.1.1. Catalyst Structure

Metallocene is a class of compounds in which cyclopentadienyl or substituted cyclopentadienyl ligands are π-bonded to the metal atom. The stereochemistry of biscyclopentadienyl (or substituted cyclopentadienyl)-metal bis (unibidentate ligand) complexes can be most simply described as distorted tetrahedral, with each η^5-L group (L = ligand) occupying a single co-ordination position, as in Figure 2.1 [11].

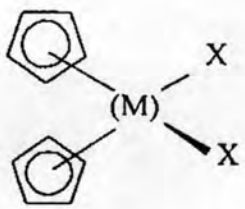

M = Zr, Hf, Ti

Figure 2.1 Molecular structure of metallocene

Representative examples of each category of metallocenes and some of zirconocene catalysts are shown in Table 2.1 and Figure 2.2, respectively.

Table 2.1 Representative Examples of Metallocenes [11]

Category of metallocenes	Metallocene Catalysts
[A] Nonstereorigid metallocenes	1) Cp_2MCl_2 (M = Ti, Zr, Hf) 2) Cp_2ZrR_2 (M = Me, Ph, CH_2Ph, CH_2SiMe_3) 3) $(Ind)_2ZrMe_2$
[B] Nonstereorigid ring-substituted metallocenes	1) $(Me_5C_5)_2MCl_2$ (M = Ti, Zr, Hf) 2) $(Me_3SiCp)_2ZrCl_2$
[C] Stereorigid metallocenes	1) $Et(Ind)_2ZrCl_2$ 2) $Et(Ind)_2ZrMe_2$ 3) $Et(IndH_4)_2ZrCl_2$
[D] Cationic metallocenes	1) $Cp_2MR(L)^+[BPh_4]^-$ (M = Ti, Zr) 2) $[Et(Ind)_2ZrMe]^+[B(C_6F_5)_4]^-$ 3) $[Cp_2ZrMe]^+[(C_2B_9H_{11})_2M]^-$ (M = Co)
[E] Supported metallocenes	1) Al_2O_3-$Et(IndH_4)_2ZrCl_2$ 2) $MgCl_2$-Cp_2ZrCl_2 3) SiO_2-$Et(Ind)_2ZrCl_2$

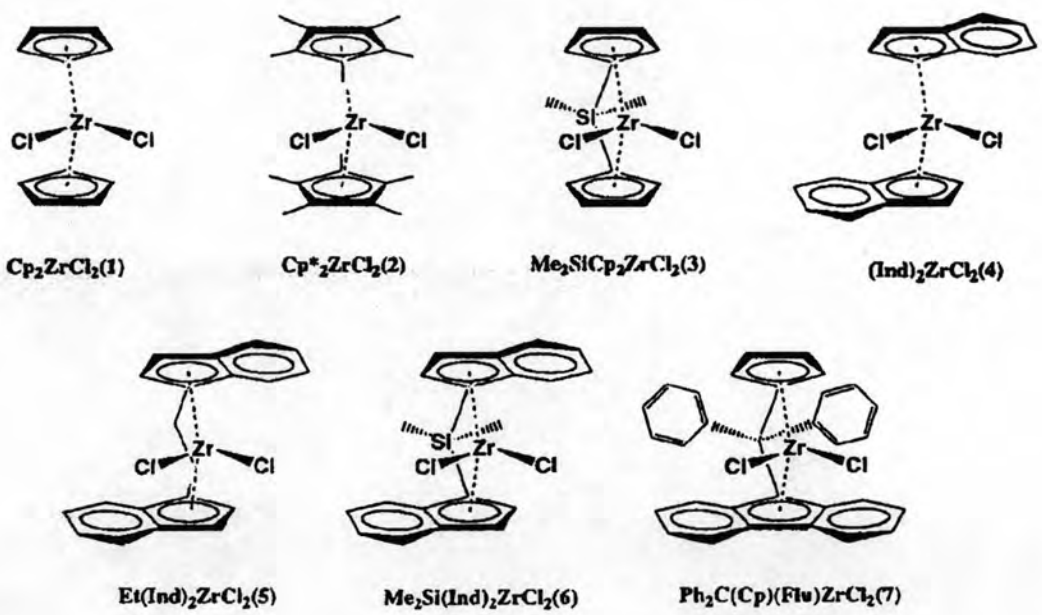

Figure 2.2 Some of zirconocene catalysts structure [12]

Composition and types of metallocene have several varieties. When the two cyclopentadienyl (Cp) rings on either side of the transition metal are unbridged, the metallocene is nonstereorigid and it is characterized by C_{2v} symmetry. The Cp_2M (M = metal) fragment is bent back with the centroid-metal-centroid angle θ about 140° due to an interaction with the other two σ bonding ligands [13]. When the Cp rings are bridged (two Cp rings arranged in a chiral array and connected together with chemical bonds by a bridging group), the stereorigid metallocene, so-called ansa-metallocene, could be characterized by either a C_1, C_2, or C_s symmetry depending upon the substituents on two Cp rings and the structure of the bridging unit as schematically illustrated in Figure 2.3[11].

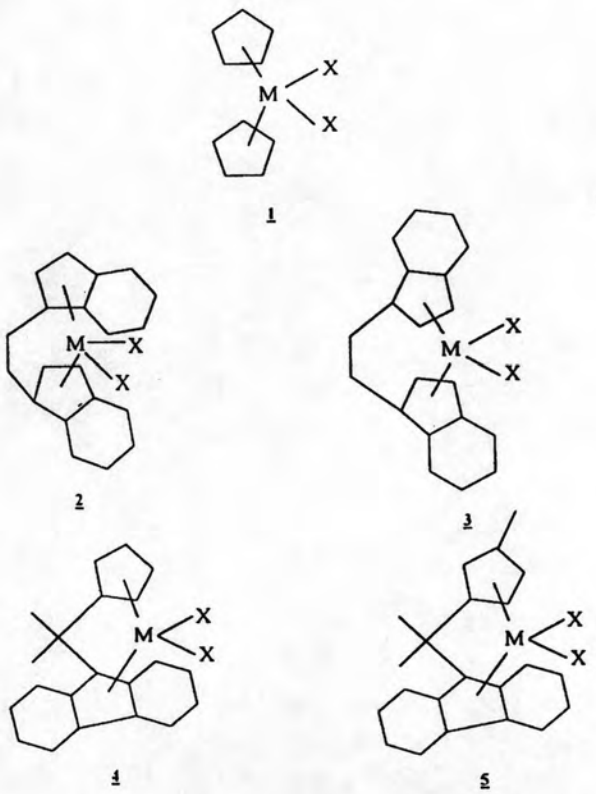

Figure 2.3 Scheme of the different metallocene complex structures [11]. Type 1 is C_{2v}-symmetric; Type 2 is C_2-symmetric; Type 3 is C_s-symmetric; Type 4 is C_s-symmetric; Type 5 is C_1-symmetric.

2.1.2. Polymerization Mechanism

The mechanism of catalyst activation is not clearly understood. However, alkylation and reduction of the metal site by a cocatalyst (generally alkyl aluminum or alkyl aluminoxane) is believed to generate the cationic active catalyst species.

First, in the polymerization, the initial mechanism started with formation of cationic species catalyst that is shown below.

Initiation

$$Et(Ind)_2ZrCl_2 + Al(CH_3)_3 \longrightarrow Et(Ind)_2ZrClMe + Al(CH_3)_2Cl$$

Propagation proceeds by coordination and insertion of new monomer unit in the metal carbon bond. Cossee mechanism is still one of the most generally accepted polymerization mechanism (Figure 2.4) [14]. In the first step, monomer forms a complex with the vacant coordination site at the active catalyst center. Then through a four-centered transition state, bond between monomer and metal center and between monomer and polymer chain are formed, increasing the length of the polymer chain by one monomer unit and generating another vacant site.

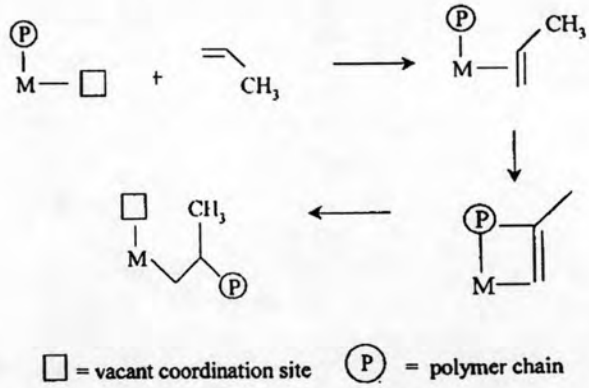

Figure 2.4 Cossee mechanism for Ziegler-Natta olefin polymerization [14].

The trigger mechanism has been proposed for the polymerization of α-olefin with Ziegler-Natta catalysts [15]. In this mechanism, two monomers interact with one active catalytic center in the transition state. A second monomer is required to form a new complex with the existing catalyst-monomer complex, thus trigger a chain propagation step. No vacant site is involved in this model. The trigger mechanism has been used to explain the rate enhancement effect observed when ethylene is copolymerized with α-olefins.

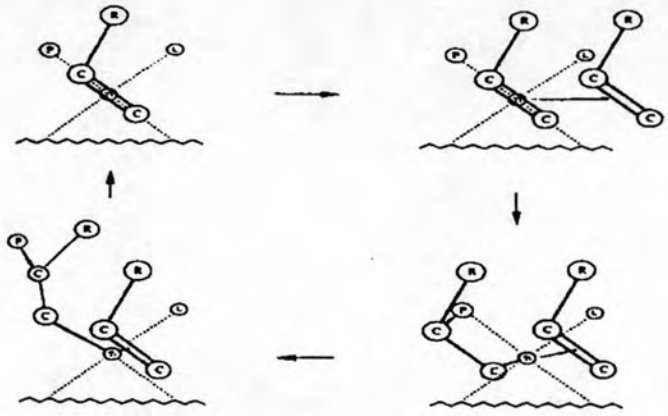

Figure 2.5 The propagation step according to the trigger mechanism [15].

After that , the propagation mechanism in polymerization shown in Figure 2.6.

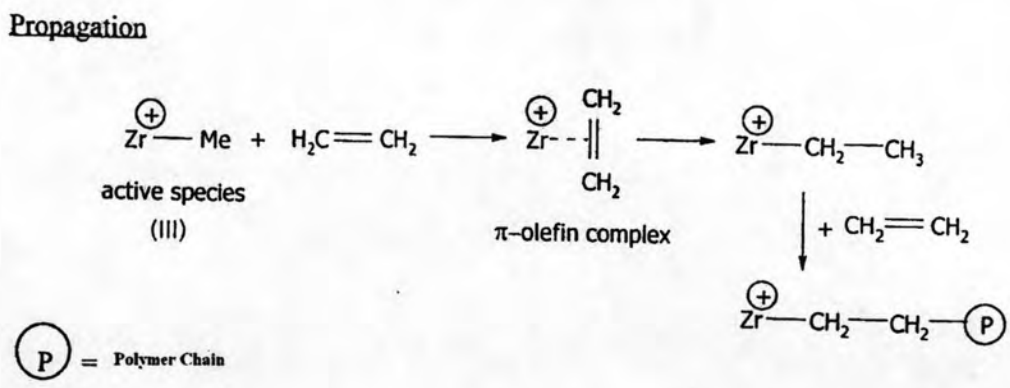

Figure 2.6 Propagation mechanism in polymerization

Finally, the termination of polymer chains can be formed by 1) chain transfer via β-H elimination, 2) chain transfer via β-Me elimination, 3) chain transfer to aluminum, 4) chain transfer to monomer, and 5) chain transfer to hydrogen (Figure 2.7-2.11)[11]. The first two transfer reactions form the polymer chains containing terminal double bonds.

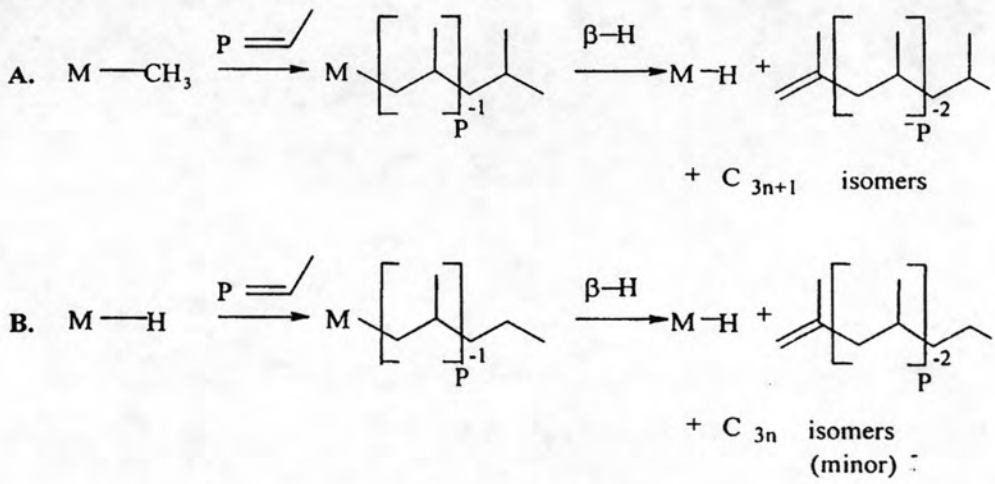

Figure 2.7 Chain transfer via β-H elimination [11]

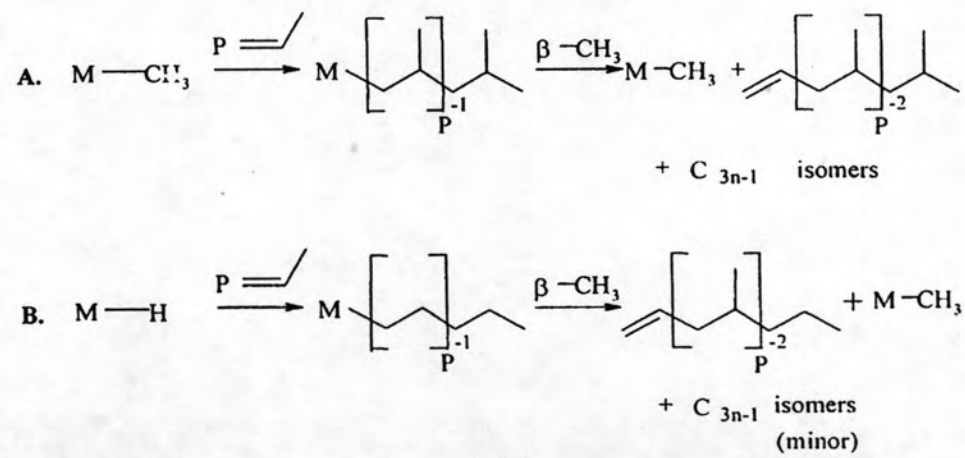

Figure 2.8 Chain transfer via β-CH_3 elimination [11]

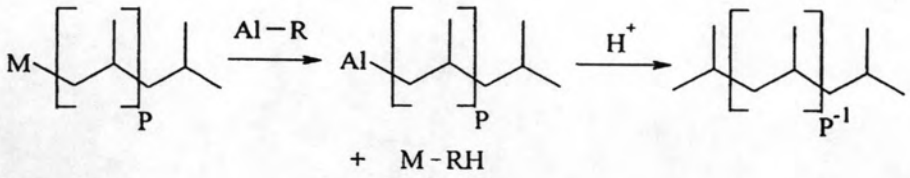

Figure 2.9 Chain transfer to aluminum [11]

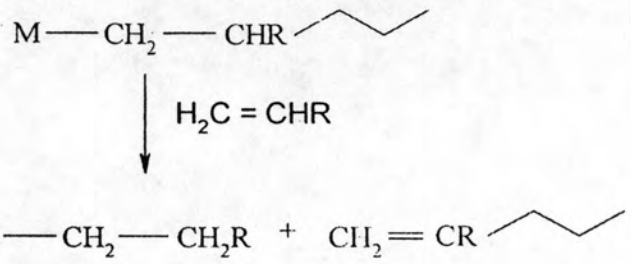

Figure 2.10 Chain transfer to monomer [11]

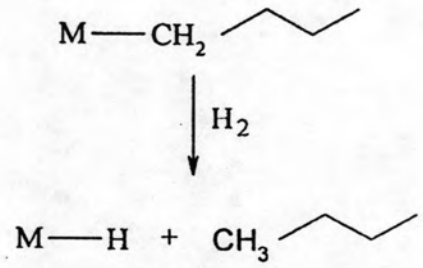

Figure 2.11 Chain transfer to hydrogen [11]

2.1.3. Cocatalysts

Metallocene catalysts have to be activated by a cocatalyst. The most common types of cocatalysts are alkylaluminums including methylaluminoxane (MAO), trimethylaluminum (TMA), triethylaluminum (TEA), triisobutylaluminum (TIBA) and cation forming agents such as $(C_6H_5)_3C^+(C_6F_5)_4B^-$ and $B(C_6F_5)_3$ [16].

Among these, MAO is a very effective cocatalyst for metallocene. However, due to the difficulties and costs involved in the synthesis of MAO, there has been considerable effort done to reduce or elimination the use of MAO. Due to difficulties in separation, most commercially available MAO contains a significant fraction of TMA (about 10-30%) [17]. This TMA in MAO could be substantially eliminated by toluene-evaporation at 25°C.

Indeed, the difficulties encountered to better understand the important factors for an efficient activation are mainly due to the poor knowledge of the MAO composition and structure. Several types of macromolecular arrangements, involving linear chains, monocycles and/or various three-dimensional structures have been successively postulated. These are shown in Figure 2.12. In recent work, a more detailed image of MAO was proposed as a cage molecule, with a general formula $Me_{6m}Al_{4m}O_{3m}$ (m equal to 3 or 4) [18].

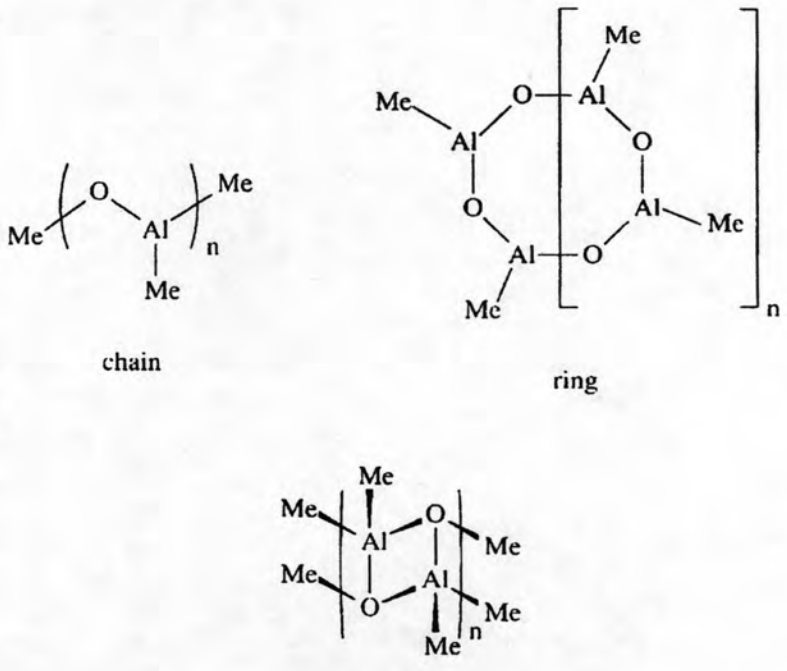

Figure 2.12 Early structure models for MAO [18]

In the case of rac-Et(Ind)$_2$ZrMe$_2$ as precursor, the extracted methyl ligands do not yield any modification in the structure and reactivity of the MAO counter-anion, thus allowing zirconium coordination site available for olefin that presented in Figure 2.13 [19].

Figure 2.13 Representation of MAO showing the substitution of one bridging methyl group by X ligand extracted from racEt(Ind)$_2$ZrCl$_2$ (X = Cl, NMe$_2$, CH$_2$Ph) [19].

Cam and Giannini [20] investigated the role of TMA present in MAO by a direct analysis of Cp$_2$ZrCl$_2$/MAO solution in toluene-d$_8$ using ^{1}H-NMR. Their observation indicated that TMA might be the major alkylating agent and that MAO acted mainly as a polarization agent. However, in general it is believed that MAO is the key cocatalyst in polymerizations involving metallocene catalysts. The role of MAO included 1) alkylation of metallocene, thus forming catalyst active species, 2) scavenging impurities, 3) stabilizing the cationic center by ion-pair interaction and 4) preventing bimetallic deactivation of the active species.

The homogeneous metallocene catalyst cannot be activated by common trialkylaluminum only. However, Soga *et al.*[21] were able to produce polyethylene with modified homogeneous Cp$_2$ZrCl$_2$ activated by common trialkylaluminum in the presence of Si(CH$_3$)$_3$OH. Their results show that for an "optimum" yield aging of the catalyst and Si(CH$_3$)$_3$OH mixture for four hours is required. However, MWD of the produced polymers is bimodal although the polymers obtained in the presence of MAO have narrow MWD.

Ethylene/α-olefins copolymers with bimodal CCD were produced with homogeneous Cp_2ZrCl_2 with different cocatalysts such as MAO and mixture of TEA/borate or TIBA/borate [22]. It seemed that the active species generated with different cocatalysts have different activities and produce polymers with different molecular weights.

2.1.4. Catalyst Activity

The ethylene polymerization rate of the copolymerization reaction with the catalyst system SiO_2/MAO/rac-Me_2Si [2-Me-4-Ph-Ind]$_2ZrCl_2$ was studied by Fink *et al.* [23]. The temperature was varied from 40 to 57°C. Small amount of hexene in the reaction solution increased the polymerization rate. The extent of the "comonomer effect" depended on the polymerization temperature. At 57°C the maximum activity of the ethylene/hexene copolymerization was 8 times higher than the homopolymerization under the same conditions. At 40°C the highest reaction rate for the copolymerization is only 5 times higher than that for the ethylene homopolymerization. For the polymer properties of the ethylene/α-olefin copolymerization, the molecular weights of the polymers decreased with increasing comonomer incorporation. Ethylene/hexene copolymers produced by a metallocene catalyst also have the same melting point and glass transition temperature.

Series of ethylene copolymerization with 1-hexene or 1-hexadecene over four different siloxy-substituted ansa-metallocene/methylaluminoxane (MAO) catalyst systems were studied by Seppala *et al.* [24]. Metallocene catalysts rac-Et[2-(t-BuMe_2SiO)Ind]$_2ZrCl_2$ (1), rac-Et[l-(t-BuMe_2SiO)Ind]$_2ZrCl_2$ (2), rac-Et[2-(i-Pr_3SiO)Ind]$_2ZrCl_2$ (3) and rac-Et[l-(i-Pr_3SiO)Ind]$_2ZrCl_2$ (4) were used. The effects of minor changes in the catalyst structure, more precisely changes in the ligand substitution pattern were studied. They found that series of polymerization with siloxy-substituted bis(indenyl) ansa-metallocene are highly active catalyst precursors for ethylene-α-olefins copolymerizations. The comonomer response of all four catalyst precursors was good. Under the same conditions the order of copolymerization ability of the catalyst was rac-Et[2-(i-Pr_3SiO)Ind]$_2ZrCl_2$ > rac-Et[2-(t-BuMe_2SiO)Ind]$_2ZrCl_2$ and rac-Et[l-(i-Pr_3SiO)Ind]$_2ZrCl_2$ > rac-Et[l-(t-

$BuMe_2SiO)Ind]_2ZrCl_2$. These catalysts are able to produce high molecular weight copolymers.

2.1.5. Copolymerization

By adding a small amount of comonomer to the polymerization reactor, the final polymer characteristics can be dramatically changed. For example, the Unipol process for linear low density polyethylene (LLDPE) uses hexene and the British Petroleum process (BP) uses 4-methylpentene to produce high-performance copolymers [25]. The comonomer can be affected the overall crystallinity, melting point, softening range, transparency and also structural, thermochemical, and rheological properties of the formed polymer. Copolymers can also be used to enhance mechanical properties by improving the miscibility in polymer blending [26].

Ethylene is copolymerized with α-olefin to produce polymers with lower densities. It is commonly observed that the addition of a comonomer generally increases the polymerization rate significantly. This comonomer effect is sometimes linked to the reduction of diffusion limitations by producing a lower crystallinity polymer or to the activation of catalytic sites by the comonomer. The polymer molecular weight often decreases with comonomer addition, possibly because of a transfer to comonomer reactions. Heterogeneous polymerization tends to be less sensitive to changes in the aluminum/transition metal ratio. Chain transfer to aluminum is also favored at high aluminum concentrations. This increase in chain transfer would presumably produce a lower molecular weight polymer. In addition, some researchers observed the decrease, and some observed no change in the molecular weight with increasing aluminum concentration [27].

The effect of polymerization conditions and molecular structure of the catalyst on ethylene/α-olefin copolymerization have been investigated extensively. Pietikainen and Seppala [28] investigated the effect of polymerization temperature on catalyst activity and viscosity average molecular weights for low molecular weight ethylene/propylene copolymers produced with homogeneous Cp_2ZrCl_2. Soga and Kaminaka [29] compared copolymerizations (ethylene/propylene, ethylene/1-hexene, and propylene/l-hexene) with $Et(H_4Ind)_2ZrCl_2$ supported on SiO_2, Al_2O_3 or $MgCl_2$.

Broadness of MWD was found to be related to the combination of support types and types of monomers. The effect of silica and magnesium supports on copolymerization characteristics was also investigated by Nowlin *et al.* [30]. Their results indicated that comonomer incorporation was significantly affected by the way that support was treated based on the reactivity ratio estimation calculated with simplified Finemann Ross method. However, it should be noted that Finemann Ross method could be misleading due to linear estimation of nonlinear system.

Copolymer based on ethylene with different incorporation of 1-hexene,1-octene, and 1-decene were investigated by Quijada [31]. The type and the concentration of the comonomer in the feed do not have a strong influence on the catalytic activity of the system, but the presence of the comonomer increases the activity compared with that in the absence of it. From ^{13}C-NMR it was found that the size of the lateral chain influences the percentage of comonomer incorporated, 1-hexene being the highest one incorporated. The molecular weight of the copolymers obtained was found to be dependent on the comonomer concentration in the feed, showing that there is a transfer reaction with the comonomer. The polydispersity (Mw/Mn) of the copolymers is rather narrow and dependent on the concentration of the comonomer incorporation.

Soga *et al.* [32] noted that some metallocene catalysts produce two-different types of copolymers in terms of crystallinity. They copolymerized ethylene and 1-alkenes using 6 different catalysts such as Cp_2ZrCl_2, Cp_2TiCl_2, Cp_2HfCl_2, $Cp_2Zr(CH_3)_2$, Et(Ind $H_4)_2ZrCl_2$ and i-Pr(Cp)(Flu)$ZrCl_2$. Polymers with bimodal crystallinity distribution (as measured by TREF-GPC analysis) were produced with some catalytic systems. Only Cp_2TiCl_2-MAO and Et(H_4Ind)$_2ZrCl_2$-MAO produced polymers that have unimodal crystallinity distribution. The results seem to indicate that more than one active site type are present in some of these catalysts. However, it is also possible that unsteady-state polymerization conditions might have caused the broad distributions since the polymerization times were very short (5 minutes for most cases).

Marques *et al.*[33] investigated copolymerization of ethylene and 1-octene by using the homogeneous catalyst system based on $Et(Flu)_2ZrCl_2$/MAO. A study was performed to compare this system with that of Cp_2ZrCl_2/MAO. The influence of different support materials for the Cp_2ZrCl_2 was also evaluated, using silica, $MgCl_2$, and the zeolite sodic mordenite NaM. The copolymer produced by the $Et(Ind)_2ZrCl_2$/MAO system showed higher molecular weight and narrower molecular weight distribution, compared with that produced by Cp_2ZrCl_2/MAO system. Because of the extremely congested environment of the fluorenyl rings surrounding the transition metal, which hinders the beta hydrogen interaction, and therefore, the chain transference. Moreover, the most active catalyst was the one supported on SiO_2, whereas the zeolite sodic mordenite support resulted in a catalyst that produced copolymer with higher molecular weight and narrower molecular weight distribution. Both homogeneous catalytic systems showed the comonomer effect, considering that a significant increase was observed in the activity with the addition of a larger comonomer in the reaction medium.

The effect of different catalyst support treatments in the 1-hexene/ethylene copolymerization with supported metallocene catalyst was investigated by Soares *et al.* [34]. The catalysts in the study were supported catalysts containing SiO_2, commercial MAO supported on silica (SMAO) and MAO pretreated silica (MAO/silica) with Cp_2HfCl_2, $Et(Ind)_2HfCl_2$, Cp_2ZrCl_2 and $Et(Ind)_2ZrCl_2$. All the investigated supported catalysts showed good activities for the ethylene polymerization (400-3000 kg polymer/mol metal.h). Non-bridged catalysts tend to produce polymers with higher molecular weight when supported on to SMAO and narrow polydispersity. The polymer produced with Cp_2HfCl_2 supported on silica has only a single low crystallinity peak. On the other hand, Cp_2HfCl_2 supported on SMAO and MAO/silica produced ethylene/1-hexene copolymers having bimodal CCDs. For the case of Cp_2ZrCl_2 and $Et(Ind)_2ZrCl_2$, only unimodal CCDs were obtained. It seems that silica-MAO-metallocene and silica-metallocene site differ slightly in their ability to incorporate comonomer into the growing polymer chain, but not enough to form bimodals CCDs.

Soares *et al.* [35] studied copolymerization of ethylene and 1-hexene. It was carried out with different catalyst systems (homogeneous $Et(Ind)_2ZrCl_2$, supported $Et(Ind)_2ZrCl_2$ and in-situ supported $Et(Ind)_2ZrCl_2$). Supported $Et(Ind)_2ZrCl_2$: an $Et(Ind)_2ZrCl_2$ solution was supported on SMAO. It was used for polymerization of ethylene and 1-hexene. In-situ supported $Et(Ind)_2ZrCl_2$: an $Et(Ind)_2ZrCl_2$ solution was directly added to SMAO in the polymerization reactor, in the absence of soluble MAO. Homogeneous $Et(Ind)_2ZrCl_2$ showed higher catalytic activity than the corresponding supported and in-situ supported metallocene catalysts. The relative reactivity of 1-hexene increased in the following order: supported metallocene ≈ in-situ supported metallocene < homogeneous metallocene catalysts. The MWD and short chain branching distribution (SCBD) of the copolymer made with the in-situ supported metallocene were broader than those made with homogeneous and supported metallocene catalysts. They concluded that there are at least two different active species on the in-situ supported metallocene catalyst for the copolymerization of ethylene and 1-hexene.

Soares *et al.* [36] investigated copolymerization of ethylene and 1-hexene with different catalysts: homogeneous $Et(Ind)_2ZrCl_2$, Cp_2HfCl_2 and $[(C_5Me_4)SiMe_2N(tert\text{-}Bu)]TiCl_2$, the corresponding in-situ supported metallocene and combined in-situ supported metallocene catalyst (mixture of $Et(Ind)_2ZrCl_2$ and Cp_2HfCl_2 and mixture of $[(C_5Me_4)SiMe_2N(tert\text{-}Bu)]TiCl_2$. They studied properties of copolymers by using ^{13}C-NMR, gel permeation chromatography (GPC) and crystallization analysis fractionation (CRYSTAF) and compared with the corresponding homogeneous metallocene. The in-situ supported metallocene produced polymers having different 1-hexene fractions, SCBD and MDW. It was also demonstrated that polymers with broader MWD and SCBD can be produced by combining two different in-situ supported metallocenes.

In addition, Soares *et al.*[37] studied copolymerization of ethylene and 1-hexene with an in-situ supported metallocene catalysts. Copolymer was produced with alkylaluminum activator and effect on MWD and SCBD was examined. They found that TMA exhibited the highest activity while TEA and TIBA had significantly lower activities. Molecular weight distributions of copolymers produced by using the

different activator types were unimodal and narrow, however, short chain branching distributions were very different. Each activator exhibited unique comonomer incorporation characteristics that can produce bimodal SCBD with the use of a single activator. They used individual and mixed activator system for controlling the SCBDs of the resulting copolymers while maintaining narrow MWDs.

2.2 Heterogeneous System

The new metallocene/MAO systems offer more possibilities in olefin polymerization compared to conventional Ziegler-Natta catalysts, such as narrow stereoregularity, molecular weight and chemical composition distributions (CCDs) through ligand design. However, only heterogeneous catalysts can be practically used for the existing gas phase and slurry polymerization processes. Without using a heterogeneous system, high bulk density and narrow size distribution of polymer particles cannot be achieved. The advantages of supporting catalysts include improved morphology, less reactor fouling, lower Al/metal mole ratios required to obtain the maximum activities in some cases the elimination of the use of MAO, and improved stability of the catalyst due to much slower deactivation by bimolecular catalyst interactions. Therefore, developing heterogeneous metallocene catalysts, that still have all the advantages of homogeneous systems, became one of the main research objectives of applied metallocene catalysis.

Steinmetz *et al.* [38] examined the particle growth of polypropylene made with a supported metallocene catalyst using scanning electron microscopy (SEM). They noticed formation of a polymer layer only on the outer surface of catalyst particles during the initial induction period. As the polymerization continued, the whole particle was filled with polymer. Particle fragmentation pattern depended on the type of supported metallocene.

2.2.1. Catalyst Chemistry

The nature of the active sites affects the polymer morphology, catalyst stability and activity, and the characteristics of the polymer produced. However, structure and chemistry of the active sites in supported catalysts are not clearly understood. Catalytic activities for supported metallocene are usually much lower than that of their counterpart homogeneous system. Formation of different active species, deactivation of catalyst during supporting procedure, and mass transfer resistance may contribute to decreased catalyst activity.

Tait *et al.* [39] reported general effects of support type, treatment, supporting procedure, and type of diluents on reaction kinetics and physical properties of polymer produced. Although the activities of supported catalysts are much lower compared to homogeneous systems. The activity of catalysts increased slightly when o-dichlorobenzene was introduced in toluene

The catalytic activities of supported catalyst depended on the percentage of the incorporated metallocene was reported by Quijada *et al.* [40]. However, in the case of metallocenes supported on MAO pretreated silica, depending on how the surface bound MAO complex with the catalyst, the activity can be as high as that of homogeneous system. According to the experiment by Chein *et al.* [41], if a single MAO is attached to silica, it would complex with zirconocene and lowers its activity. On the other hand, if multiple MAOs are attached to the surface silanol, the supported zirconocene will not be further complexed with MAO and have activity.

2.2.2. Supporting Methods

In the case of carriers like silica or other inorganic compounds with OH group on the surface, the resulting catalyst displayed very poor activities even combined with MAO. The reaction of metallocene complexes with the Si-OH groups might cause the decomposition of active species. Such decomposition could be suppressed by fixing MAO on the silica surface and then reacting with metallocenes [42]. Therefore, silica must be pretreated before the interaction with metallocene, to reduce the OH concentration and to prepare an adequate surface for metallocene adsorption and reaction in a non-deactivating way [43]. Metallocene immobilization

methods can be divided in to three main groups. The first method is the direct support of catalyst onto an inert support. The second method involves the pretreatment of the inert support with MAO or other alkylaluminum followed by metallocene supporting. The third method, the catalyst is chemically anchored to the support, which often involves in-situ catalyst synthesis. These methods produce catalysts with distinct activities, comonomer reactivity ratios, and stereospecificities.

2.3 Polymer nanocomposites

From the many previous study results ,we observe that different composite systems can lead to very different results. One important observation is that composites with nano-sized inclusions generally have different properties than composites with larger scale inclusions [44]. The specific reasons why the polymer matrix composites with nano-sized reinforcement have different properties than composites with micron-sized reinforcement are not fully understood, but several theories have been introduced to explain some of the changes in material morphology and behavior that are seen at the nano-scale. It is important to point out, however, that most of these theories were developed to explain particular results and, therefore, are not necessarily applicable to a large number of polymer nanocomposites.

Chan et al. [45] proposed that properties such as elastic modulus, tensile strength, and yield strength decrease in nanocomposites with polypropylene matrix due to the change in nucleation caused by the nanoparticles (Fig.2.14). The nanoparticles produce a much larger number of nucleating sites but, in turn, greatly reduce the size of these spherulites. In their experimental work, no spherulites were found in the nanocomposites by SEM indicating that either none were present or they were reduced to such a small size that SEM could not detect them. It was further proposed that there was another mechanism which was causing these same properties to increase. The increase occurred when there was a strong interaction between the polymer and filler. This interaction had larger impact in nanocomposites due to the large interfacial area between the filler particles and the matrix.

Other investigators have suggested that this interaction leads to a layer of polymer that is directly adsorbed and bound to the particles [46,47,48,49]. Experimental work that has been performed on a polystyrene-cobalt nanocomposite with cobalt nanoparticles with an average size of 21 nm has shown that the polymer layer was about 24 nm, and varied non-linearly with molecular weight [50].

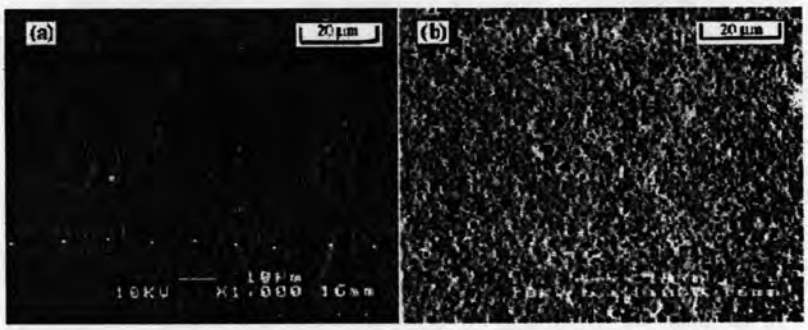

Figure 2.14 (a) Pure polypropylene (b) polypropylene with 9.2% volume filler [45].

An increase in yield and tensile strength and modulus in nanocomposite systems as compared to microcomposites can be partially explained on the basis of the interaction between the filler and the matrix. It has been found that a greater adhesion between the matrix and inclusion causes less debonding when a stress is applied and, consequently the elastic modulus and strength are improved [51].

Vollenberg and Heikens [46] explained that if there is a strong interaction between the polymer and the particle, the polymer layer in the immediate proximity of the particle will have a higher density. For most systems, density is proportional to elastic modulus, so the region directly surrounding the inclusions will be a region of high modulus. The polymer right outside this high modulus region will have a lower density due to the polymer chains that are moved towards the particle. For large particles, the size of the low density region will be relatively large, and the contribution of the high modulus filler will be diminished. For nanoparticles, the number of particles for a given volume fraction is much larger, thus the particles will be much closer to one another. If the particles are densely packed, then the boundary

layer of polymer at the interface will comprise a large percentage of the matrix and can create a system where there is no space for a low modulus region to form. This results in the elastic modulus of composites with smaller particle size (nano) being greater than the modulus of composites with larger inclusions [46,47].

The small interparticle distance in nanocomposites was used as another parameter to explain the changes in the elastic modulus and strength of these materials when compared with the composites with micron-sized particles. The same parameter also plays a role in the glass transition temperature changes observed in nanocomposites versus composites with micron-sized reinforcement. Ash et al. [49] found that for their system the glass transition temperature was constant until around 0.5% weight fraction of particles, then had a sharp drop, and then it remained constant for weight fractions above 1%. When there is little or no interfacial interaction between the filler and matrix and the interparticle distance is small enough, the polymer between two particles acts as a thin film. For a thin film, the glass transition temperature decreases as film thickness decreases. The distance between particles in a composite with the filler weight fraction below 0.5% is relatively large, and hence, in this case the polymer between each particle is not considered to belong to the thin film regime. As the filler concentration increases, the interparticle distance and the resulting thickness of the film, decrease. This theory, however, does not explain why the glass transition temperature levels off rather than continues to drop as a function of increasing weight fraction of the filler. A drop-off in Young's modulus was found for the same filler weight fraction as the drop in glass transition temperature. It was proposed that as the glass transition temperature decreased, the relative testing temperature increased. Also, the elastic modulus of the matrix, PMMA, decreases as temperature increases, so the drop in glass transition temperature is correlated with the drop in modulus [48,49].

Reynaud et al. [52] found that during tensile testing, the volume of polymer nanocomposites increased, with the greatest increase occurring in systems with the smallest particles. To explain this, the debonding process of the polymer next to the inclusions was examined, as shown in Fig. 2.15. It was proposed that the smallest particles tend to aggregate and debonding occurs around each individual

particle. As a result, the large clusters of small particles act as larger soft particles. On the other hand, the larger filler particles do not aggregate and each particle undergoes a single debonding process.

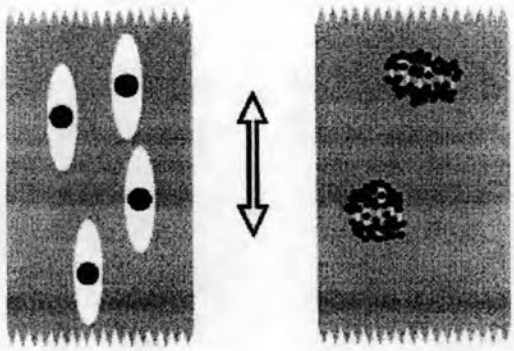

Figure 2.15 Debonding around 50 and 12 nm particle [52].

Due to the different results obtained and the different nature of the various polymer nanocomposite systems, there is no observed universal trend that can be modeled and explained.

There are, however, observations that show the behavior of nanocomposites different from composites with larger scale inclusions. The particle size and the polymer and particle morphology tend to play a very important role. In addition, the nature of dispersion and aggregation of particles can affect the properties of composites significantly. Filler–matrix interaction is another factor that influences the properties. The strength of the interaction plays a role in the thickness and density of the interphase, which consists of a layer of high density polymer around the particle. The effects of the interface on the behavior of a composite depend upon the interparticle distance. For constant filler content, with reduction in particle size, number of filler particles in-creases, bringing the particles closer to one another. Thus, the interface layers from adjacent particles overlap, altering the bulk properties significantly. These issues play a major role in the effect of nano-sized inclusions in a polymer matrix. For nanoparticles, any configuration changes in the matrix will have

a significant effect when the characteristic radius of polymer chains is of the same order as the inclusions [51,53]. There are other areas addressed in literature.

For example, L´opez et al. [54] examined the processing and thermal and mechanical properties of magnetic nanocomposites. In another work the mechanical properties of clay nanocomposites were analyzed as a function of filler loading and orientation [55]. Zhang et al. [56] provided a look at matrix–filler interfacial properties. Effect of matrix on the polymer matrix composites were examined by Friedlander et al. [57].

2.4 Linear low density polyethylene (LLDPE) nanocomposites

Although the high amount of nanocomposite researches have done ,there still have the low amount of them relating to LLDPE. The adequately experimental made by some researchers include here.

Hotta and Paul [58] studied L-clay nanocomposites . It was prepared by melt compounding various combinations of a maleic anhydride grafted linear low density polyethylene (LLDPE-g-MA), a linear low density polyethylene (LLDPE), and two organoclays. The two types of organoclay were selected to show the effect of the number of alkyl groups attached to the nitrogen of the organic modifier on exfoliation and improvement of mechanical properties. Nanocomposites derived from the organoclay having two alkyl tails, M2(HT)2, exhibited better dispersion and improvement of mechanical properties than nanocomposites based on the organoclay having one alkyl tail M3(HT)1. This result is the opposite of what is observed for nylon-6 nanocomposites. In addition, the rheological properties and gas permeability of the nanocomposites derived from the organoclay having two alkyl tails, M2(HT)2 were investigated. Both melt viscosity and melt tension (melt strength) increased with increased content of clay (MMT) and LLDPE-g-MA. Gas permeability was decreased by the addition of MMT.

Ki Hyun Wang et al. [59] studied maleic anhydride grafted polyethylene (maleated polyethylene)/clay nanocomposites prepared by simple melt compounding. The exfoliation and intercalation behaviors depended on the

hydrophilicity of polyethylene grafted with maleic anhydride and the chain length of organic modifier in the clay. When the number of methylene groups in alkylamine (organic modifier) was larger than 16, the exfoliated nanocomposite was obtained, and the maleic anhydride grafting level was higher than about 0.1 wt% for the exfoliated nanocomposite with the clay modified with dimethyl dihydrogenated tallow ammonium ion or octadecylammonium ion. The pure LLDPE showed only the intercalation, which does not depend on the initial spacing between clay layers.

Lew et al. [60] studied LLDPE-organoclay nanocomposites containing a synthetic tetrasilisic fluoromica prepared from metallocene-catalyzed and conventional Ziegler-Natta-catalyzed linear low-density polyethylenes (LLDPE) by means of melt-compounding. The effects of maleic-anhydride grafted compatibilizer (PE-g-MA) level, clay concentration, and blending procedure were investigated and compared. Morphology and structural analysis using transmission electron microscopy (TEM) and X-ray diffraction (XRD) suggested the clay exfoliation was more intense in the metallocene LLDPE matrix, conceivably because of the controlled short-chain branching and viscosity effects. When exfoliated, these silicate sheets were shown to restrict the lamellar crystallization, as seen by the decrease in crystallinity using differential scanning calorimetry analysis (DSC). The dynamic mechanical thermal analysis (DMTA) study suggested that the three α ,β and γ –relaxations of the LLDPE were affected by polymer chain branching and clay exfoliation level.

Sometime LLDPE was used as a form of blending polymer to investigate the properties of nanocompossites. Tsu-Hwang Chuang et al. [61] blended ethylene-vinyl acetate copolymer (EVA)/montmorillonite (MMT) composite with a linear low density polyethylene (LLDPE). X-ray diffraction and transmission electron microscopy (TEM) image of the EVA/MMT composite are in support of an intercalated with partially delaminated nanocomposite. The tensile strength of the nanocomposite is about 20% higher than that without layered silicates, MMT. Furthermore, the incorporation of MMT into polymer blend delays the main thermo-oxidative degradation. Cone calorimeter test points out that the addition of layered silicates into the pristine EVA/LLDPE blend or the blend with a low smoke

non-halogen (LSNH) fire retardants, aluminum trihydroxide, and antimony trioxide, can reduce the maximum heat release rate by 30–40%. The smoke suppressing effect of layered silicates is only observed in the nanocomposite containing flame retardants. According to the limiting oxygen index (LOI) data and cone calorimeter test, the addition of the nanodispersed layered silicate and LSNH flame retardants to the EVA/LLDPE exhibits a synergistic effect on the flame retardancy and smoke suppression.

2.5 Alumina nanocomposites

In heterogeneous polymerization research field, many inorganic supports such as Al_2O_3, SiO2and $MgCl_2$ have been investigated. It was reported that Al_2O_3 is perhaps the most attractive support so far. Beside be the excellent support, Alumina also be claimed to be the excellent filler in the polymer composites. To fill the alumina into polymer matrix, melting method and solution mixing method is more favor than in situ polymerization in the present time. However the in situ polymerization was found to be the promising method.

Benjamin J. Ash et al [62] investigated mechanical properties of Al_2O_3/polymethylmethacrylate (PMMA) nanocomposite alumina /polymethylmethacrylate. The particle were dispersed using sonication and the composite were polymerized using free radical polymerization. At an optimum weight percent, the resulting nanocomposites showed, on average, a 600% increase in the strain-to-failure and the appearance of a well-defined yield point when tested in uniaxial tension. Concurrently, the glass transition temperature (Tg) of the nanocomposites dropped by as much as 25 °c, while the ultimate strength and the Young's modulus decreased by 20% and 15%, respectively. For comparision, composites containing micron size alumina particles were synthesized and displayed neither phenomenon.

Rui Yang et al [63] studied the photo-degradation of linear low density polyethylenes (LLDPE) modified with inorganic nano-fillers and/or light stabilizers by Fourier transform infrared spectroscopy (FTIR). The results indicated that all the

nano-fillers used-Al2O3, SiO2 and ZnO-had positive effect on the photo-stabilization of LLDPE. Among them, ZnO had the best effect, while Al_2O_3 the least. The influence mechanism of these three fillers was also discussed. The combination of two nano-particles had worse stabilization effect compared to a single nano-particle, which means unsynergism between fillers. Two light stabilizers, SPN and 6911, had different influences on the photo-oxidation of LLDPE. Compared to SPN, 6911 was a better antioxidant; that is to say, all the samples with 6911 had no evident photo-oxidation during the exposure time. Besides, the photo-oxidation in the surface is more than twice of that in the bulk.

M.C. Kuo et al [64] studied the poly (ether-ether-ketone) (PEEK) polymer filled with nano-sized silica or alumina measuring 15–30 nm to 2.5–10 wt% are fabricated by vacuum hot press molding at 400 ˚C. The resulting nanocomposites with 5–7.5 wt% SiO_2 or Al_2O_3 nanoparticles exhibit the optimum improvement of hardness, elastic modulus, and tensile strength by 20–50%, with the sacrifice of tensile ductility.With no surface modification for the inorganic nanoparticles, the spatial distribution of the nanoparticles appears to be reasonably uniform. There seems no apparent chemical reaction or new phase formation between the nanoparticle and matrix interface. The crystallinity degree and thermal stability of the PEEK resin with the addition of nanoparticles are examined by X-ray diffraction, differential scanning calorimetry, and thermogravity analyzer, and it is found that a higher crystallinity fraction and degradation temperature would result in the composites as compared with the unfilled PEEK.

M.C. Kuo et al [65] investigated on the non-isothermal crystallization kinetic behaviors have been conducted by means of differential scanning calorimeter. The Avrami, Ozawa, and combined Avrami and Ozawa equations were applied to describe the crystallization kinetics and to determine the crystallization parameters of the alumina-filled PEEK nanocomposites. It is found that the inclusion of the nano-sized alumina particles can accelerate the nucleation rate due to heterogeneous nucleation but reduce the growth rate due to retarded polymer chain mobility. The resulting crystal grain size appears to be smaller in the nanocomposites. On the other hand, the nanocomposites show a higher Avrami value than that of the neat PEEK, implying a

more complex crystallization configuration. Moreover, the combined Avrami and Ozawa equation can successfully describe the crystallization model under the non-isothermal crystallization.

Praveen Bhimaraj et al. [66] studied the friction and wear properties of poly (ethylene) terephthalate (PET) filled with alumina nanoparticles. The nanoparticle loading was varied from 1 to 10 wt%. The nanocomposite samples were tested in dry sliding against a steel counterface. The results show that the addition of nanoparticles can increase the wear resistance by nearly 2× over the unfilled polymer. The average coefficient of friction also decreased in many cases. The nanocomposites form a more adherent transfer film that protects the sample from the steel counterface, although the presence of an optimum filler content may be due to the development of abrasive agglomerates within the transfer films in the higher wt% samples. This study varied both crystallinity and weight percent of filler in a PET matrix in an attempt to separate the effects of nanofillers and crystallinity on the tribology.